International Journal of Engineering and Technical Research (IJETR)
ISSN: 2321-0869 (O) 2454-4698 (P) Volume-7, Issue-10, October 2017

Designing PID Controller for STATCOM a SVC in Multi-machine System Using Modal Theory Method

Nguyen Huu Vinh, Nguyen Hung, Le Kim Hung

***Abstract*— In this paper, the comparative simulation results of using a static synchronous compensator (STATCOM) and a static VAR compensator (SVC) to achieve damping enhancement of a three-machine system is presented. PID damping controllers of the proposed STATCOM and SVC are designed by using Modal Theory Method to contribute adequate damping characteristics to the dominant modes of the studied system. A frequency-domain approach using eigenvalue analysis and a time-domain scheme based on a nonlinear system model subject to a three-phase short-circuit fault at the load connected bus are systematically performed to examine the effectiveness of the proposed control schemes. It can be concluded from the comparative simulated results that the designed PID damping controller joined with the proposed STATCOM is shown better than the proposed SVC.**

***Index Terms*— Static Synchronous Compensator (STATCOM), static VAR compensator, Multi-machine System, Stability.**

I. INTRODUCTION

Nowadays, flexible AC transmission systems (FACTS) devices are proposed to implement to power grid for improving the stability of the systems. In which, a new topology structure of a static VAR compensator (SVC), i.e., a low-cost improved thyristor-controlled reactors by removing series circuit elements, proposed in [1] was used to correct the unbalanced problems and improve the reliability of power systems. As well as, a hybrid SVC presented in [2] was utilized to improve reactive power control capability of wind farms fed to an AC grid in case of low-voltage conditions. A SVC and a thyristor-controlled series compensator (TCSC) were employed in a single-machine infinite-bus system to improve transient voltage stability of an asynchronous wind farm [3]. A SVC was located at the middle point of the tie line to damp out inter-area oscillations occurred in a two-area four-machine system [4, 5]. Comparing to the performance of a SVC, a static synchronous compensator (STATCOM) gave a larger contribution to transient margin and low-voltage ride-through capability of squirrel-cage induction generator-based wind farms using both calculations and simulations [6]. In [7], a STATCOM was connected at the point of common coupling to maintain stable voltage and to improve the power quality by protecting doubly fed induction generator (DFIG)-based wind farm connected to a weak grid from going offline during and after disturbances. As proposed in [8], a new control strategy using a full-power wind permanent-magnet generator (PMG) with a STATCOM to provide reactive power compensation can be used to improve stability of transient voltage. In [9], performance of a PMG-based wind energy system employing a dynamic voltage regulator was compared to one of the system employing a STATCOM. It is recommended to use a STATCOM in systems with large loads where reactive power consumption from the grid could cause serious effects on connected loads.

This paper presents a STATCOM/SVC and load is connected to a point of common coupling (PCC). They compensate reactive power at the connected bus and maintaining the voltage at PCC. The main case study in this paper is to design PID controllers for STATCOM and SVC to improve oscillations of the studied system.

Nguyen Huu Vinh, he is now with the Ho Chi Minh City Power Corporation, Vietnam

Nguyen Hung, he is with Faculty of Electrical, Mechanical and Electronics Ho chi minh City University of Technology, Vietnam

Le Kim Hung, he is now with Electrical Engineering, University of Science and Technology, The University of Danang, Vietnam

II. SYSTEM CONFIGURATION AND MATHEMATICAL MODELS

Fig. 1 shows the configuration of the studied system. A STATCOM/SVC with capacity of 20MVA is connected to Bus 5 of a three-machine power system.

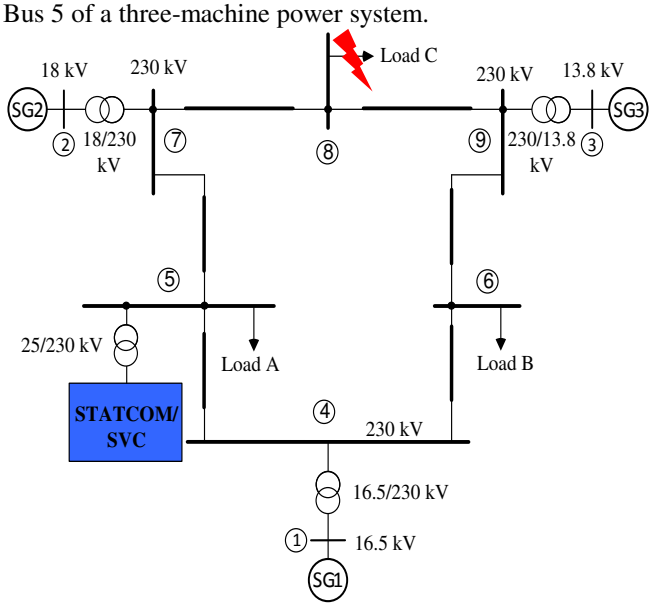

Fig. 1. Configuration of the studied system

The mathematical models of the synchronous generator (SG), STATCOM, SVC, network and there pu differential equations are presented in subsection below.

A. Synchronous Generator Model [10]

The well-known three-machine nine-bus power system which is widely used in power system stability studies was shown in Fig. 1. The complete parameters of this system and reference frame can be found in [10]. In this case study, the SG_i model is represented by a two-axis model as block diagram that is shown in Fig. 2. In this model, the transient effects are accounted for while the transient effects are neglected.

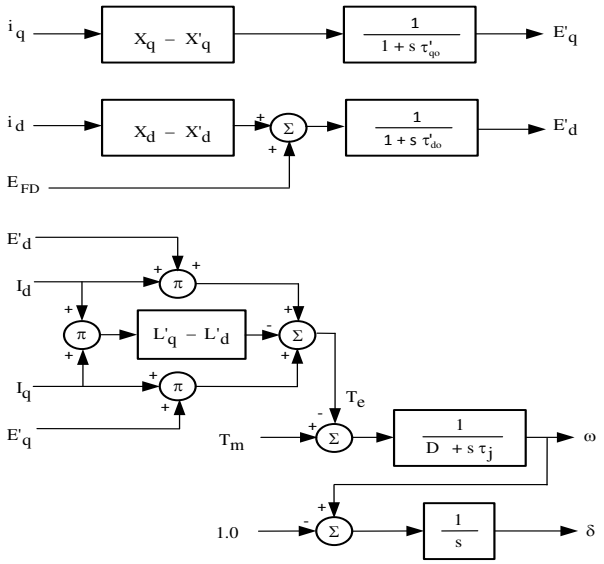

Fig. 2. Block diagram of the two-axis SG model.

The pu differential equations for the *i*-th synchronous generator are described as below.

$$p(E'_{di}) = \frac{1}{\tau'_{qoi}}\left[-E'_{di} - \left(X_{qi} - X'_{qi}\right)I_{qi}\right] \quad (1)$$

$$p(E'_{qi}) = \frac{1}{\tau'_{doi}}\left[-E'_{qi} + E_{FDi} + \left(X_{di} - X'_{di}\right)I_{di}\right] \quad (2)$$

$$p(\omega_i) = \frac{1}{\tau_{ji}}\left[T_{mi} - \left[I_{di}E'_{di} + I_{qi}E'_{qi} - \left(L'_{qi} - L'_{di}\right)I_{di}I_{qi}\right] - D_i\omega_i\right] \quad (3)$$

$$p(\delta_i) = \omega_i - 1 \quad (4)$$

where:

δ_i (rad) and ω_i (rad/s) represent the rotor angular position and angular velocity, respectively;

E'_{di} (pu) and E'_{di} (pu) are the internal transient voltages of the synchronous generator, respectively;

E_{FDi} (pu) is the field voltage;

I_{di} (pu) and I_{qi} (pu) are the d- and q-axis currents;

τ'_{doi} (s) and τ'_{qoi} (s) are the d- and q-open-circuit transient time constants;

X'_{di} (pu) and X'_{qi} (pu) are the d- and q- transient reactance;

X_{di} (pu) and X_{qi} (pu) are the d- and q- synchronous reactance;

T_{mi} (pu) is the mechanical nominal torque;

D_i is the damping factor;

B. Multi-Machine System [10]

Fig. 3 presents the studied multi-machine system. This network has three synchronous generators and three loads. Assume that the three loads are represented by three constant impedances while three generators are represented by three active sources. Therefore, all the nodes have zero injection currents except for the generator nodes.

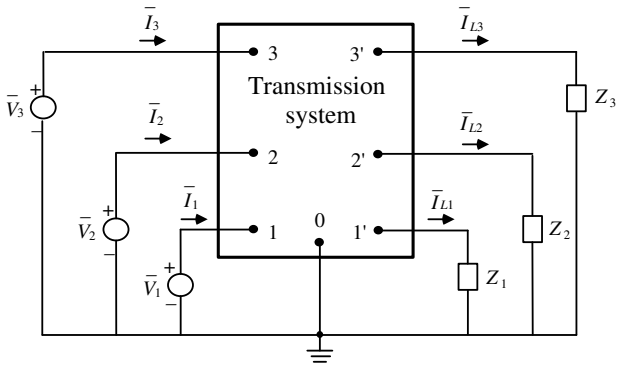

Fig. 3. Multi-machine system with constant impedance loads

This property is used to obtain the network reduction as shown below. With the relation between nodal currents and voltages is:

$$\mathbf{I}_{sys} = \bar{\mathbf{Y}}_{sys}\mathbf{V} \quad (5)$$

or

$$\begin{bmatrix}\mathbf{I}_3 \\ \hline \mathbf{0}\end{bmatrix} = \left[\begin{array}{c|c}\mathbf{Y}_{31} & \mathbf{Y}_{32} \\ \hline \mathbf{Y}_{33} & \mathbf{Y}_{34}\end{array}\right]\begin{bmatrix}\mathbf{V}_{31} \\ \hline \mathbf{V}_{32}\end{bmatrix} \quad (6)$$

where

$\mathbf{I}_3 = \begin{bmatrix}\bar{I}_{L1} & \bar{I}_{L2} & \bar{I}_{L3}\end{bmatrix}^{\mathrm{T}}$ is the injected current vector at generator nodes,

$\mathbf{V}_{31} = \begin{bmatrix}\bar{V}_1 & \bar{V}_2 & \bar{V}_3\end{bmatrix}^{\mathrm{T}}$ is the voltage vector at the generator nodes,

$\mathbf{V}_{32} = \begin{bmatrix}\bar{V}_{1'} & \bar{V}_{2'} & \bar{V}_{3'}\end{bmatrix}^{\mathrm{T}}$ is the voltage vector at the eliminated nodes,

$\bar{\mathbf{Y}}_{sys}$ is the original system admittance matrix. In this case, $\bar{\mathbf{Y}}_{sys}$ is the desired reduced matrix and it has the dimensions of 3×3.

Expanding the above equations, it yields:

$$\mathbf{I}_3 = \mathbf{Y}_{31}\mathbf{V}_{31} + \mathbf{Y}_{32}\mathbf{V}_{32} \quad (7)$$

$$\mathbf{0} = \mathbf{Y}_{33}\mathbf{V}_{31} + \mathbf{Y}_{34}\mathbf{V}_{32} \quad (8)$$

From these (7) and (8) equations, V_{32} can be eliminated to get:

$$\mathbf{I}_3 = \left(\mathbf{Y}_{31} - \mathbf{Y}_{32}\mathbf{Y}_{34}^{-1}\mathbf{Y}_{33}\right)\mathbf{V}_{31} \quad (9)$$

$$\bar{\mathbf{Y}} = \left(\mathbf{Y}_{31} - \mathbf{Y}_{32}\mathbf{Y}_{34}^{-1}\mathbf{Y}_{33}\right) \quad (10)$$

Because of each SG is modeled under its own *qd*-axis reference frame rotating with its rotor, we can transform from generator's *qd*-axis rotor reference frame to the common *QD*-axis reference frame as follows:

$$\begin{bmatrix}i_{Qi} \\ i_D i\end{bmatrix} = \begin{bmatrix}\cos\delta_i & \sin\delta_i \\ \sin\delta_i & -\cos\delta_i\end{bmatrix}\begin{bmatrix}i_{qi} \\ i_{di}\end{bmatrix} \quad (11)$$

$$\begin{bmatrix}v_{Qi} \\ v_D i\end{bmatrix} = \begin{bmatrix}\cos\delta_i & \sin\delta_i \\ \sin\delta_i & -\cos\delta_i\end{bmatrix}\begin{bmatrix}v_{qi} \\ v_{di}\end{bmatrix} \quad (12)$$

C. STATCOM Model

The single line diagram of the employed STATCOM is presented in Fig. 4. The relationship between output voltage of the STATCOM and its parameters can be written by [6,7]:

$$v_{dsta} = V_{dcsta}.km_{sta}.\sin(\theta_{PCC} + \alpha_{sta}) \quad (13)$$

$$v_{qsta} = V_{dcsta}.km_{sta}.\sin(\theta_{PCC} + \alpha_{sta}) \quad (14)$$

where

v_{qsta} and v_{dsta} are the pu q- and d-axis voltages at the output terminals of the STATCOM, respectively;

km_{sta} and α_{sta} are, respectively, the modulation index and phase angle of the STATCOM;

θ_{PCC} is the voltage phase angle of the common AC bus;

V_{dcsta} is the pu DC voltage of the DC capacitor Cm.

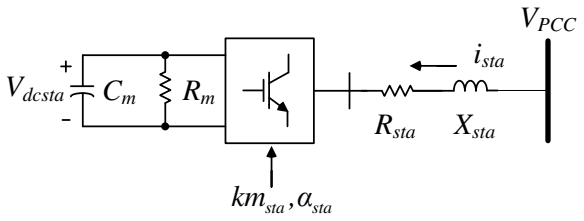

Fig. 4. Single-line diagram of the employed STATCOM

The pu DC voltage, current equations of the DC capacitor C_m can be described by

$$p(V_{dcsta}) = \frac{\omega_b}{C_m}\left(I_{dcsta} - \frac{V_{dcsta}}{R_m}\right) \quad (15)$$

$$I_{dcsta} = i_{qsta}.km_{sta}\cos(\theta_{PCC} + \alpha_{sta}) + i_{dsta}.km_{sta}\sin(\theta_{PCC} + \alpha_{sta}) \quad (16)$$

where

I_{dcsta} is the pu DC current flowing into the positive terminal of V_{dcsta};

R_m is the pu equivalent resistance considering the equivalent electrical losses of the STATCOM

i_{qsta} and i_{dsta} are the pu q- and d-axis currents flowing into the terminals of the STATCOM, respectively.

Fig. 5 presents the fundamental control block diagram of the STATCOM with the PID controllers. The pu DC voltage V_{dcsta} is controlled by α_{sta} while the AC voltage v_{sta} is varied by changing km_{sta}.

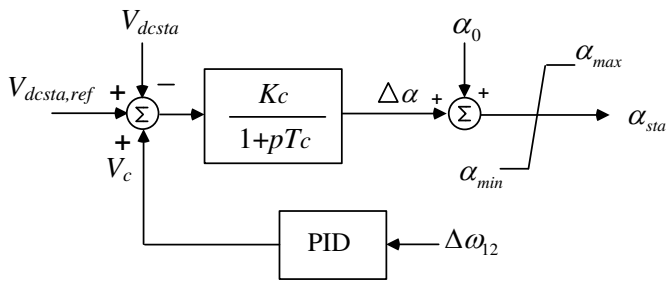

Fig. 5. Control block diagram of the STATCOM

D. Static VAR Compenstor (SVC) Model [4]

In this paper, the proposed SVC is referenced from [4]. Its single line diagram of the SVC with TCR-FC components type was presented in Fig. 6. The voltage at the PCC is adjusted by injecting the reactive power into system from SVC.

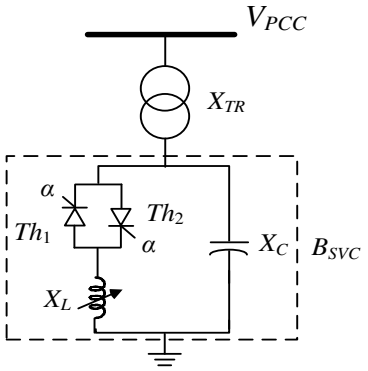

Fig. 6. One-line diagram of the SVC

Fig. 7 shows the control block diagram of the studied SVC. When the voltage at PCC is lower than the reference voltage, the value of B_{SVC} of the SVC is positive to inject reactive power to the system. When the voltage at PCC is higher than the reference voltage, the B_{SVC} of the SVC is negative to absorb reactive power from the power system. Assuming a balanced and fundamental-frequency operation, the equivalent B_{SVC} of the SVC is a function of the firing angle α as shown below [6].

$$B_{SVC}(\alpha) = \frac{2\alpha - \sin(2\alpha) - \pi\left(2 - \frac{X_L}{X_C}\right)}{\pi X_L} \quad (17)$$

where X_L and X_C are reactance of reactor and capacitor of SVC, respectively.

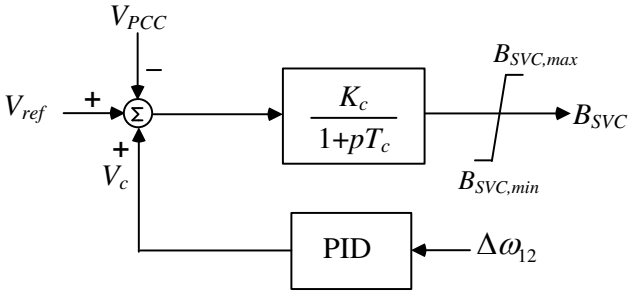

Fig. 7. Control block diagram of the SVC

III. Design PID Controller Of Statcom And Svc Using Modal Control Theory

This subsection describes the design procedure and design results of the PID damping controllers for the proposed STATCOM and SVC to achieve stability improvement of the studied system using pole placement technique. The nonlinear system equations are linearized around a selected nominal operating point to acquire a set of linearized system equations in matrix form of [10]

$$p(\mathbf{X}) = \mathbf{AX} + \mathbf{BU} + \mathbf{VW} \quad (18)$$

$$\mathbf{Y} = \mathbf{CX} + \mathbf{DU} \quad (19)$$

where **X** is the state vector, **Y** is the output vector, **U** is the external or compensated input vector, **W** is the disturbance input vector while **A**, **B**, **C**, and **D** are all constant matrices of appropriate dimensions.

The eigenvalues of the studied three-machine nine-bus system are listed in the second column of Table I. In which, the

eigenvalues from modes 1 to 10 relate to the modes of the three-machine nine-bus. It can be found by examining the system eigenvalues listed in the second column of Table 1 that all modes of the system are almost fixed on the complex plane and the modes 1 and 2 relating to the rotor angle deviation between SG#1 to SG#2 ($\Delta\delta_{12}$) and the rotor angle deviation between SG#1 to SG#3 ($\Delta\delta_{13}$), respectively, are changed and these modes can be improved by damping controllers.

Table I. Eigenvalues of the studied system

Modes	System	System with STATCOM and PID	System with SVC and PID
1	**-0.57 ± *j*15.69**	**-0.8 ± *j*13.0**	**-0.8 ± *j*13.0**
2	**-0.72 ± *j*8.62**	**-1.0 ± *j*8.0**	**-1.0 ± *j*8.0**
3	-5.26 ± *j*7.88	-5.27 ± *j*7.89	-5.26 ± *j*8.02
4	-5.24 ± *j*7.94	-5.28 ± *j*7.93	-5.34 ± *j*7.96
5	-5.37 ± *j*7.96	-5.38 ± *j*7.97	-5.24 ± *j*7.94
6	-3.53 ± *j*1.11	-7.43 ± *j*0.78	-0.44 ± *j*0.77
7	-0.45 ± *j*0.82	-0.32 ± *j*0.88	-0.37 ± *j*0.57
8	-0.37 ± *j*0.53	-0.37 ± *j*0.65	-0.27 ± *j*0.20
9	-0.24 ± *j*0.03	-0.18 ± *j*0.15	-2.03, -4.69
10	-0.14, -3.22	-0.24, -3.23	-0.41, -2.42
11	-6.91	-1.69, -0.23	-6.71, -0.14
12	-	-100.02, -99.40	-26.71, -13.71
13	-	-0.33 ± *j*0.18	-7.36 ± *j*14.25
14	-	-3.71	-3.23

The control block diagrams of the proposed STATCOM and SVC including the designed PID damping controllers were shown in Fig. 5 and Fig. 7, respectively. The PID damping controller senses the rotor speed deviation of the SG#1 and SG#2 ($\Delta\omega_{12}$) to generate a damping signal (V_c) in order to improve the damping ratios of modes 1 and 2 of studied system. Hence, the output signal in (19) is $\mathbf{Y} = \Delta\omega_{12}$ and $\mathbf{U} = V_c$ is the input vector. The transfer function H(p) of the PID controller for the STATCOM/SVC is given by

$$H(p)=\frac{\mathbf{U}(p)}{\mathbf{Y}(p)}=\frac{V_c(p)}{\Delta\omega_{12}(p)}=\frac{pT_w}{1+pT_w}\left(K_P+\frac{K_I}{p}+pK_D\right) \quad (19)$$

where p is the Laplace operator; T_w is the time constant of the wash-out term; K_P, K_I, and K_D are the proportional gain, integral gain, and derivative gain of the damping controller, respectively.

For improving the damping of the selected modes, in this studied system, two new eigenvalues are selected as (-0.8 ± *j*13.0) and (-1.0 ± *j*8.0) for mode 1 and mode 2, respectively. The design results of the PID damping controller for the STATCOM are given as K_P = 32.5, K_I = 83.4, K_D = 23.4, and T_W = 0.4 s, and the design results of the PID damping controller for the SVC are given as K_P = 17.7, K_I = 127.5, K_D = -4.3, and T_W = 0.5 s. The new eigenvalues of the studied system and the proposed STATCOM and SVC joined with the designed PID damping controllers are listed in the third and the fourth columns of Table I. In which, the modes of the proposed STATCOM/SVC and the designed PID damping controllers are from 11-14. It can be clearly observed that modes 1 and 2 have been exactly positioned on the desired locations on the complex plane.

IV. Time Domain Simulations Of Nonlinear Model

In this section, time domain simulations are performed by using the nonlinear system model developed in the previous section to compare the damping characteristics contributed by the proposed STATCOM and SVC joined with the designed PID damping controllers on stability improvement of the studied system under a three-phase short-circuit fault happened at the load C belong to Bus 8 of Fig. 1.

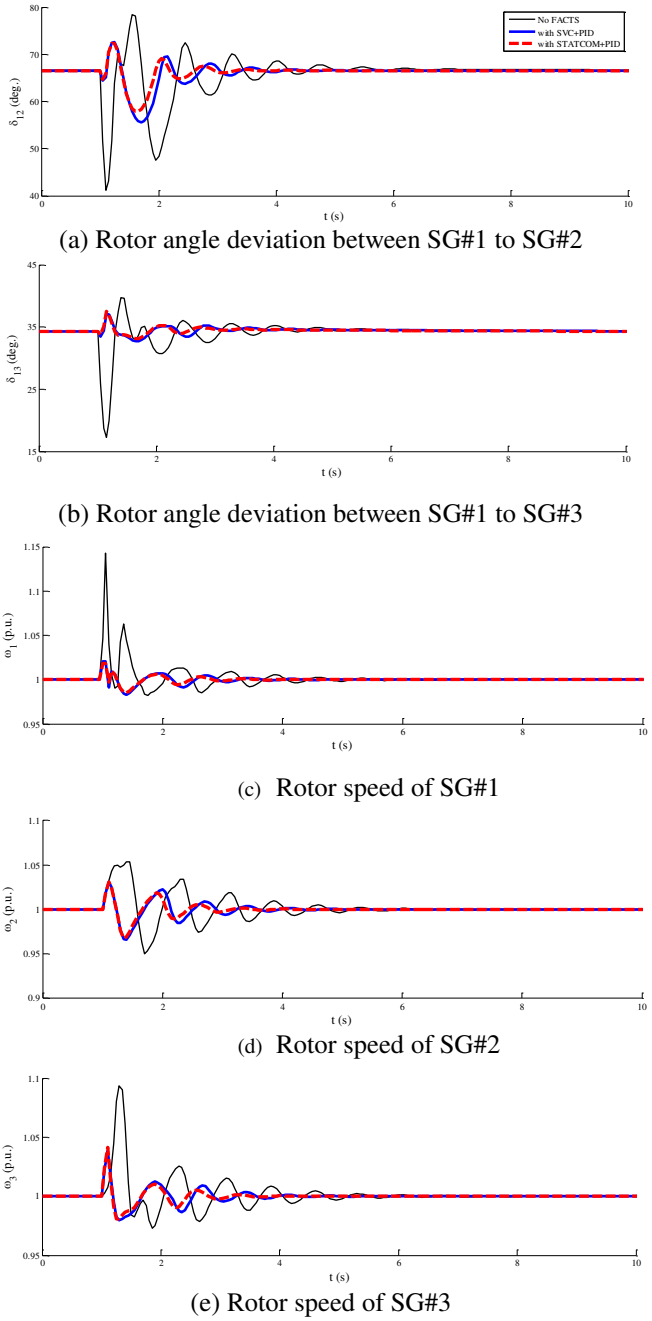

(a) Rotor angle deviation between SG#1 to SG#2

(b) Rotor angle deviation between SG#1 to SG#3

(c) Rotor speed of SG#1

(d) Rotor speed of SG#2

(e) Rotor speed of SG#3

Fig. 8. Transient responses of the studied system under a three-phase short-circuit fault at load C

The three-phase short-circuit fault is suddenly happened at t = 1 s and is cleared after 5 cycles. The simulation results of the proposed system using MATLAB/SIMULINK toolbox are presented in Fig. 8. In this figure, the comparative transient responses of the studied system without FACTS devices **(black lines)**, with the SVC and PID damping controller

(blue lines), and with the STATCOM and PID damping controller **(red dotted lines)** are respectively plotted. In which, the rotor angle derivation of the SG#1 to SG#2 and SG#1 to SG#3 are shown in Fig. 8(a) and Fig. 8(b), respectively. The rotor speeds of three SGs are also shown in Figs. 8(c)-(e). It is clearly observed from the comparative transient simulation results that the proposed STATCOM joined with the designed PID damping controller can offer better damping characteristics than the SVC joined with the designed PID damping controller. This is due to the fact that the maximum capacitive power generated by a STATCOM decreases only linearly with the bus voltage but it drops off as square of the bus voltage for a SVC.

V. CONCLUSION

This paper has presented the comparative stability improvement studied of a multi-machine system using a STATCOM and a SVC. To supply the adequate reactive power to the system, PID damping controllers for the proposed STATCOM and SVC have been designed by using pole placement technique to assign two dominant modes of the studied system to the desired locations on the complex plane. Comparative time-domain simulations of the studied system subject to a three-phase short-circuit fault at the other load bus have been systematically performed to demonstrate the effectiveness of the proposed STATCOM and SVC joined with the designed damping controllers. Since a STATCOM provides faster control than an SVC and improved control range, it can be concluded from the simulation results that the proposed STATCOM joined with the designed controller has better damping characteristics to improve the performance of the studied multi-machine system under a severe operating condition

REFERENCES

[1] Z. Yu, Z. Jianhua, Z. Aiguo, "A novel topology structure of SVC based on energy saving for unbalanced three phase compensation in low voltage power system," in *Proc. IEEE Region 10 TENCON Conference,* 2009, pp. 1-5.

[2] P. Vuorenpaa and P. Jarventausta, "Enhancing the grid compliance of wind farms by means of hybrid SVC," in *Proc. IEEE PowerTech*, 2011, pp. 1-8.

[3] Z. Hua, W. Hongfen, Q. Xiaoyan, X. Jian, W. Xiwen, and W. Song, "Improvement of transient voltage stability of the wind farm using SVC and TCSC," in *Proc. Power and Energy Engineering Conference (APPEEC)*, 2011, pp. 1-4.

[4] Y. Chang, Z. Xu, G. Chen, and J. Xie, "A novel SVC supplementary controller based on wide area signals," in *Proc. IEEE Power Engineering Society General Meeting*, 2006, pp.1-7.

[5] A. Jalilvand and M.D. Keshavarzi, "Adaptive SVC damping controller design, using residue method in a multi-machine system," in *Proc. 6th Int. Conf. on Electrical Engineering/Electronics, Computer, Telecommunications and Information Technology*, 2009, pp.160-163.

[6] M. Molinas, J.A. Suul, and T. Undeland, "Low voltage ride through of wind farms with cage generators: STATCOM versus SVC," *IEEE Trans. Power Electronics*, 2008; 23(3), pp. 1104-1117.

[7] B. Pokharel and W. Gao, "Mitigation of disturbances in DFIG-based wind farm connected to weak distribution system using STATCOM," in *Proc. North American Power Symposium (NAPS)*, 2010, pp. 1-7.

[8] G. Cai, C. Liu, Q. Sun, D. Yang and P. Li, "A new control strategy to improve voltage stability of the power system containing large-scale wind power plants," in *Proc. 4th Int. Conf. Electric Utility Deregulation and Restructuring and Power Technologies (DRPT)*, 2011, pp. 1276-1281.

[9] M.N. Eskander and S.I. Amer, "Mitigation of voltage dips and swells in grid-connected wind energy conversion systems," in *Proc. ICCAS-SICE*, 2009, pp. 885-890.

[10] P.M. Anderson and A.A. Fouad, *Power System Control and Stability*, Iowa: The Iowa State University Press, Ames, 1977

Nguyen Huu Vinh was born in Vietnam. He received the B.S. and M.S. degrees from Electrical and Electronics Engineering Department of Ho Chi Minh City University of Technology, Viet Nam in 2001 and 2009 respectively. He is now working for Ho Chi Minh City Power Corporation,Vietnam. His research fields include Power System Operation, FACTS, Power Quality

Nguyen Hung was born in Vietnam. He received the B.S. and M.S. degrees from Electrical and Electronics Engineering Department of Ho Chi Minh City University of Technology, Viet Nam in 2000 and 2004 respectively. He then received the Ph.D degree from Pukyong National University, Korea, in 2010. He is currently a lecturer with HUTECH Institute of Engineering, HUTECH University of Technology, Vietnam. His research interests include FACTS, Power System Operation and Renewable Energy

Le Kim Hung was born in Vietnam. He is currently a professor with Faculty of Electrical Engineering, University of Science and Technology, The University of Danang, Vietnam. His research interests include FACTS, Power System Protection and Renewable Energy